Al-Rafidain Journal of Computer Sciences and Mathematics (RJCSM)

www.csmj.mosuljournals.com

An Advanced GAN-Based Framework for Medical Image Enhancement

Saja Younis Hamid Alhamdani

Department of Artificial Intelligence, College of Computer Science and Mathematics, University of Mosul, Iraq
Email: sata@uomosul.edu.iq

Article information

Article history:
Received 1 June, 2025
Revised 25 July, 2025
Accepted 17 August, 2025
Published 25 December, 2025

Keywords:
Image Enhancement,
Medical image,
GAN algorithm.

Correspondence:
Saja Younis Hamid Alhamdani
Email: sata@uomosul.edu.iq

Abstract

Low contrast, noise, and low visual detail are major medical image problems that pose a negative effect on diagnostic accuracy. This paper suggests a more developed model using deep generative networks (GANs) to enhance the quality of medical iris images. The framework has a sequence of preprocessing steps that include contrast enhancement (CLAHE), noise removal (Bilateral Filter), and edge enhancement (Unsharp Masking), and then the stage of enhanced generation with an attention-assisted generator (Adam) with fine-tuned parameters. SSIM, PSNR and LPIPS measures were used to evaluate the performance of the model. The findings revealed that there were significant visual and perceptual structure of images as results showed that, average SSIM was improved by 0.9383 to 0.9783, LPIPS was reduced by 0.0137 to 0.0078 and PSNR had increased by 28.62 to 32.23 than the default parameters. These results confirm the usefulness of fine-tuning at enhancing perceptual and structural image measures. This model improves the diagnosis abilities in the medical field and minimizes the use of costly refined imaging methods, hence it can be applied in large scale clinical setting.

DOI: 10.33899/rjcsm.v19i2.60304,

I. Introduction

Modern healthcare clinicians are extensively dependent on medical imaging not only in diagnosis but also in treatment planning in a variety of specialties, and a solid body of image data, collected using a variety of heterogeneous devices, makes a significant contribution to patient safety and diagnostic accuracy [1]. Acquisition apparatuses (medical imaging) in the field use sensors to transform the invisible textural characteristics of density, contrast, and reflectance into measurable digital intensities which are captured to generate a diagnostic image [2].

Imaging technologies have developed fast and widened the opportunities of seeing the human anatomy in a way it has never been seen before. Medical imaging is nowadays unavoidable in every sector of healthcare, including nuclear, computed tomography, magnetic resonance imaging, and others. These methods will produce different modalities of images which will have to be considered and reproduced in the most effective way to obtain best diagnostic results [3]. Better and more accurate software is a key component of a comprehensive data analysis and assessment tool.

Due to the unavailability of image enhancement technologies in the medical field, diagnostic images often suffer from reduced brightness, contrast, and clarity, which impairs the quality of medical imaging and makes diagnosis difficult, especially in complex medical cases [4] [5].

Image enhancement is a procedure of improving the quality of an image; sometimes, this refers to restoration or reconstruction [6]. Enhancement consists of both image sharpening (via a Laplace filter) and image smoothing (using a Gaussian blur filter) to enhance contrast while preserving edge details and minimizing noise [7]. Image smoothing generally is an operation that reduces the prominence of the variation of tone concerning the local average [8].

Most smoothing operations act to suppress high frequencies, which correspond to detail, so the operation is sometimes referred to as low-pass filtering. In image processing, an image may be degraded or corrupted, or too much noise may be added. Many existing restoration techniques fail to give satisfactory results in the presence of

noise [9]. Simple schemes such as averaging filters, Wiener filters, or Kalman filters can be very effective when designed to work with low, wide-band Gaussian noise. However, they all fail in the presence of heavy noise and other non-Gaussian noise distributions [10].

Image enhancement algorithms are a crucial tool in enhancing the efficiency and accuracy of medical image analysis. They improve image characteristics, making it easier for physicians to detect pathological details, increasing the reliability of clinical assessment and decision-making effectiveness [11]. The enhancement algorithms for digital images have been studied earlier to improve their quality. However, most of the methods are based on classical approaches such as histogram equalization, contrast stretching, etc. [12]. They usually focus on enhancing their contrast and brightness.

Recently, with the blooming of artificial intelligence research interests, as skill gaps have been reduced between humans and computers [13], It has been observed that there has been a rapid development of image enhancement algorithms based on neural networks. Currently, deep neural networks have been widely used in numerous applications ranging from natural image processing to all optical, acoustic, and radar-systems related inverse-scatterings and reconstructions [14]. Among the neural network architectures, Generative Adversarial Networks (GANs) have shown exceptional promise in medical image enhancement tasks. GANs consist of two competing networks—a generator and a discriminator—that learn through adversarial training to produce high-fidelity images [5]. Despite their success, many existing models rely on default training parameters.

Based on the above challenges in medical image quality and visual detail accuracy, this research aims to develop an advanced framework based on deep generative networks (GANs) to enhance medical iris images in terms of contrast, noise reduction, and fine detail enhancement. A series of preprocessing steps is adopted, followed by an improved generation model that incorporates spectral normalization in the discriminator to address instability during training our model, which helps control gradient magnitudes and stabilizes the adversarial learning process.

The above method is supported by the Adam initialization algorithm and optimal choice of hyperparameters, thus balancing visual performance and computational performance. This paper attempts to address this gap in this contribution, evaluating the effect of hyperparameter optimization on the quality of GAN - generated medical images. As well as intend to support the effectiveness of the suggested model through a quantitative analysis using SSIM, PSNR, and LPIPS metrics that are combined to measure the improvements that have been made to the final images.

2. Related Work

Deep generative adversarial networks (GANs) are an extremely promising technology that can be used to improve medical imagery in recent years due to the ability to restore small visual details and improve the overall quality of images with low resolutions or noise. These degradations can often be due to natural constraints of imaging equipment, or even deliberate degradation of radiation dose. Among the most remarkable of the pieces in this field: In a study by Mahboubisarighieh et al. [15], To improve the fidelity of medical radiographic images, researchers have come up with a generative adversarial network (GAN)-based framework. The architecture has used a perceptual learning algorithm and been applied to dental radiographs, with a significant increase in image clarity. The quantitative evaluation resulted in structural similarity index (SSIM) of ≈ 0.848, maximum signal to noise ratio (PSNR) of 25.46 dB, and learned perceptual image patch similarity (LPIPS) value of ≈ 0.152. The results testify to the effectiveness of the model in comparison with the traditional approaches; however, they cannot be rated as the best outcomes that are necessary to achieve high-quality diagnostic imaging. Abdusalomov et al. [16] The authors offered a proposal which is based on the model of the SRGAN to sharpen the medical images in low-light settings, addressing the issues of fine details recovery and image quality improvement. The research has assessed the performance of the model based on objective measures, such as PSNR and SSIM, and the values are 28.45 0 dB and 0.8423, respectively.These results indicate acceptable effectiveness of the model, but they still fall short of the ideal performance required for high-resolution medical images.

3. Technical Background

3.1. Image Preprocessing Techniques

Noises often distort images. Noise is an unwanted disturbance that generally occurs while capturing photos or when the image is transmitted from one channel to another. [17]. The atmosphere of the image affects it due to various reasons, such as blurriness, pixelization, brightness, etc. To eliminate this noise, add some distortion to itself, which is generally termed as noise, and the removal of this noise is a crucial task, and it depends on the noisy image; with this original image, it can be regenerated [18].

Image Denoising. Depending on the application, an image filter may need to enhance features of interest and/or reduce those that contain noise. Such applications are particularly useful in medical imaging, remote sensing, photographic display, and archiving [19]. Several filtering techniques have been proposed for this purpose. These schemes may be categorized as either linear or nonlinear procedures. Linearity refers to operations in which the output pixel, such as an arithmetic mean, can be computed directly as a linear view of a subset of pixel values centered about the target pixel. With linear filters, such as Gaussian filters, the gray values of filtered images are a linear combination of the original quantities. The

constraints of linearity are such that the output of an input function is a function only of a linear combination of its components. Nonlinear methods represent pixel values in terms of a nonlinear function [20] [21].

3.2. CLAHE

Contrast is an essential feature of an image. An image will appear more natural, more stunning, and transmit more detail and information if the contrast in the photo is more reasonable or optimal. Contrast enhancement for enhancing the visual appearance of a distorted image is one of the leading research problems in digital image processing [22]. A widely adopted example is contrasting limited adaptive histogram equalization (CLAHE), which performs local adjustments in image contrast with low noise amplification [23]. These contrast adjustments are interpolated between patches of neighboring images called kernels. CLAHE achieves spatial adaptivity through the selection of kernel size. The intensity range of the kernel histogram, set by a clip limit, restrains noise amplification [24] [25].

3.3. Bilateral filtering noise reduction

A bilateral filter is a nonlinear filtering technique for image processing. It is a noniterative and edge-preserving filter that replaces the value of a pixel, which is only what it makes of itself and the surrounding pixels, with a weighted average of its spatial neighbors [6] [26]. It has been used in image denoising to eliminate noise while preserving edges in photographs, and in computer graphics to maintain sharpness in 2D and 3D images [27] [28].

3.4. Sharpening via unsharp masking

The unsharp masking technique is a popular image processing technique for enhancing sharpness in photographic images [29]. The method employs a technique in which an enhanced frame is obtained by superimposing a blurred image and an enhanced image that are derived from a reference image [30]. Mathematical models of the information loss in a Gaussian blurring process, as well as the ringing artifacts produced in the unsharp masking method, have been formulated [31].

3.5. Generative Adversarial Networks (GANs)

Generative Adversarial Networks (GANs) are now very famous in the machine learning community and are a very popular model for image generation tasks. In its early stage, GANs were adapted to the medical imaging area to generate medical images for a moderately sized dataset [32]. The key idea of GANs is to train a generator and a discriminator; the generator creates fake images to confuse the discriminator. In contrast, the discriminator attempts to tell apart which images have real labels and which ones are fake. The two networks confront each other, and their performances improve with each iteration. Eventually, when the generator is sufficiently improved, it can generate realistic images that are indistinguishable from real ones [33], As in **Figure 1**. GANs are appropriate for cases when insufficient real data is a problem, as they generate additional fake data. Besides, GANs have an advantage over other image synthesis approaches since GANs explicitly learn distributions of the underlying training sample data rather than explicitly modeling the image signal formation process [34] [35].

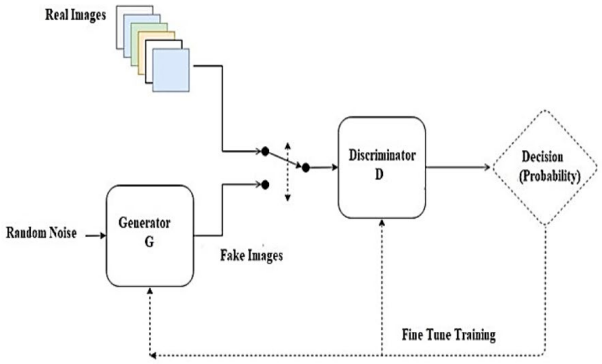

Figure 1. Schematic Block Diagram of Generative Adversarial Network (GAN) [33].

3.6. Evaluation Metrics

To maintain and control the quality of an image using image compression systems or to enhance the quality of the image using image enhancement systems, it is essential to assess the image's quality. Since quality assessment is directly related to the ability of the observer to discriminate between signal and noise, an accurate quality assessment is generally required to be subjectively measured. [36]. The Human Visual System (HVS) is the final recipient of any visual information, and its knowledge plays a vital role in constructing accurate models for measuring image quality.

Structural Similarity Index Measure (SSIM): Structural Similarity Index (SSIM) is a perceptually motivated measure of the quality of a visual signal, where the range is between -1 and 1, and it is equal to 1 if the two images are the same [37]. The mathematical formulation for the standard implementation mode of SSIM is given together with theoretical proofs of the definition of the quality index and the constants used to prevent divisions by zero [38].

Learned Perceptual Image Patch Similarity (LPIPS): There are several thorough investigations into the flaws of existing deep perceptual similarity metrics and the properties of human perception [39]. The perceptual similarity of image patches is tightly linked to their semantic similarity [40]. Dimensions perceptually judged by humans can be challenging to learn from simple data reduction techniques. (LPIPS) It is a neural-network-based perceptual metric that compares deep feature activations across image patches. It correlates more

closely with human judgments of similarity compared to traditional pixel-level metrics [41].

Peak Signal-to-Noise Ratio (PSNR): Peak Signal-to-Noise Ratio (PSNR) is a widely used metric in image processing, particularly for assessing image coding algorithms, and it is used to measure the quality of reconstructed images by comparing the peak signal value of the ground truth image with the super-resolution algorithm's error. PSNR is commonly used to assess the performance of SR algorithms due to its computational efficiency and ease of implementation [42].

4. Methodology

Our methodology, as shown in Figure2, it illustrates the sequential stages of the proposed system, starting from the initial setup to the final evaluation and saving of results. The pre-processing phase incorporates three enhancement techniques — Contrast Limited Adaptive Histogram Equalization (CLAHE), Bilateral Filtering, and Unsharp Masking — to improve image clarity before passing the data to the Model and training phase and then to the evaluation and saving phase.

4.1. Pre-processing phase: began with a comprehensive preprocessing phase aimed at preparing the medical iris images for deep learning enhancement. Each image was first converted to grayscale and resized to ensure compatibility with convolutional architectures. To improve local contrast while preserving fine details, CLAHE was applied. Noise reduction was handled using a brilliant bilateral filtering technique, which effectively removed noise without sacrificing important structural features. To further highlight critical details, a sharpening filter was applied, resulting in more transparent and more diagnostic images.

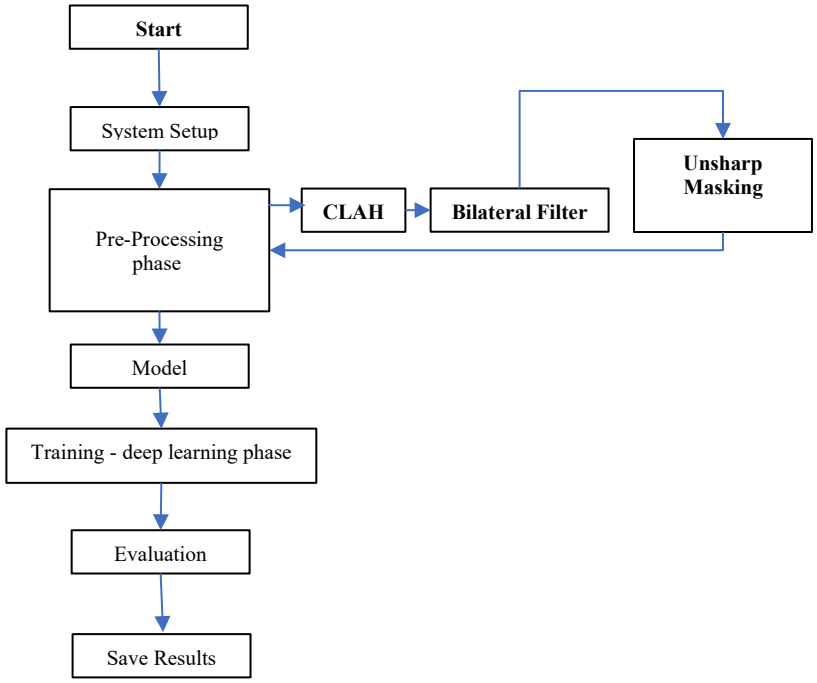

Figure 2. Flowchart of the proposed medical image enhancement framework.

4.2. Model and training phase: In this phase, the pre-processed medical images are fed into a custom-designed deep learning model built upon a generative architecture integrated with spectral normalization to stabilize the training of the discriminator and prevent exploding gradients, In this paper was applied spectral normalization to all convolutional layers within the discriminator network, by doing so, the discriminator's learning becomes more stable and the GAN training process converges more reliably [43], whereas, an attention mechanism that is integrated into the generator to help the network focus on anatomically relevant regions, enhancing detail preservation in critical areas of medical images. **Figure 3** showing the training pipeline begins by loading image batches, followed by generating enhanced images and calculating both **L1 loss** and **VGG perceptual loss**, which are then combined. Backpropagation is performed, and the model parameters are updated using the **Adam optimizer**, which was configured with custom hyperparameters *(learning rate = 0.0003, $\beta_1 = 0.7$, $\beta_2 = 0.999$)* to improve convergence stability and training efficiency. The process repeats itself many times in a sequence of epochs, utilizing early stopping to prevent overfitting. The model of excellence is automatically maintained upon achieving the ideal performance. Such arrangement allows the generator to enhance image quality in

a series of steps, at the same time preserving structural integrity and reducing the occurrence of artifacts and distortions.

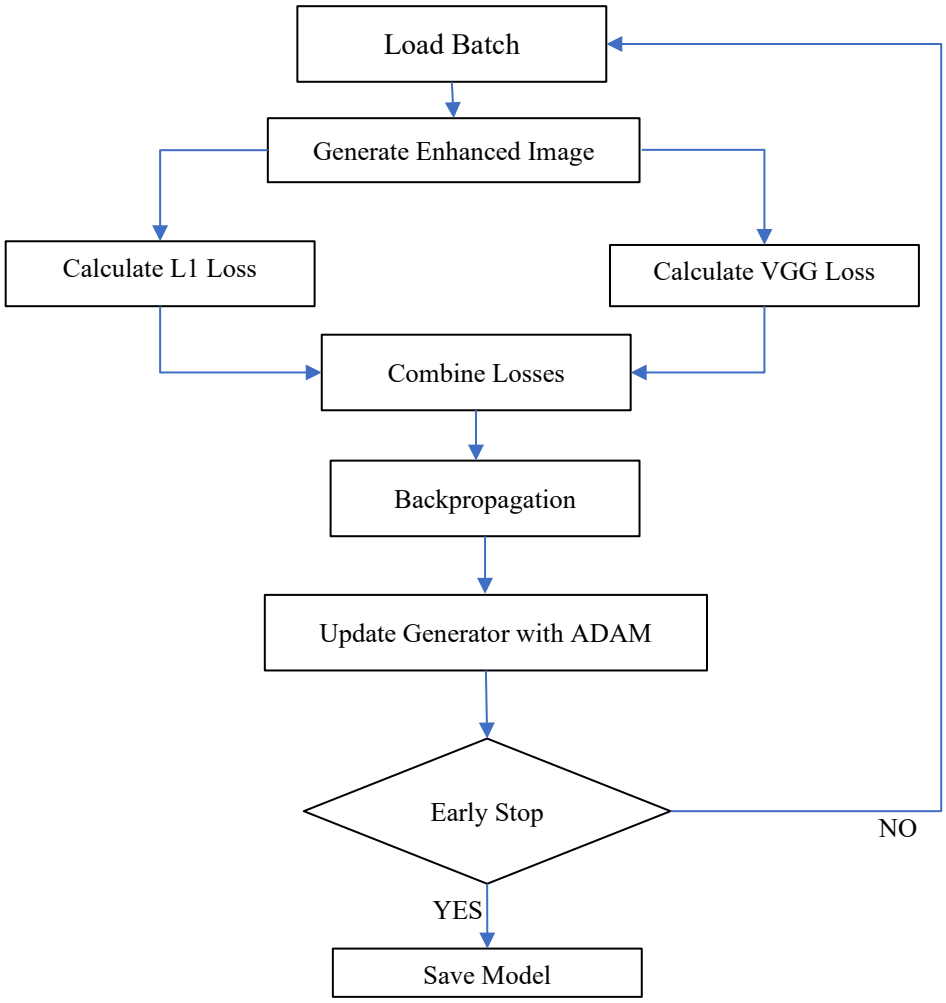

Figure 3. Overview of the Deep Learning Training Workflow Using GAN-Based Generator.

Optimizer Configuration in Deep Learning: Adam with Custom Hyperparameters

Training of the model was done using the Adam optimization algorithm (Adaptive Moment Estimation) and early stopping was implemented to prevent overfitting. The arrangement of Adam used included learning rate of 0.0003, β_1 and β_2 momentum coefficients of 0.7 and 0.999, respectively. The chosen learning rate of 0.0003 is sufficiently small to encourage slow but steady weight changes and therefore the risk of divergence throughout the learning process is reduced. β_1=0.7 is the first momentum coefficient, which defines the exponent decay rate of the gradient mean, which reduces the effect of antecedent gradients, and eliminates overshoot of local minima. On the other hand, β_2 = 0.999 determines the decay rate of squared gradients, which allows the dynamically adjusting of learning rates according to the parameter. Such a large B2 value allows robust processing of sparse or noisy gradients, especially a beneficial attribute in processes that require finer-tuning.

4.3. Evaluation and Saving Phase: Undertake a thorough evaluation of model performance in the end of training using a set of objective metrics related to performance which include Structural Similarity Index (SSIM), Peak Signalto Noise Ratio (PSNR), and Learned Perceptual Image Patch Similarity metric (LPIPS). These measures are used to measure the visual and structural fidelity of the processed images to their raw images. To supplement these numerical assessments, also maintain qualitative visual assessments so that can make perceptual inspections. Moreover, every incremental step of the image-enhancement process is stored, and this enables a visual record of the steps which facilitates transparency and reproducibility.

This research is based on the publicly available "Iris Database" by M. Dobeš and L. Machala (2002) [44], which was

obtained from an online source and consists of 384 iris images taken from 64 individuals. Each person was photographed three times on the right side of the body and three times on the left side, catching three images of the right eye and three of the left eye respectively. This was done to give the variety of lighting and image capture conditions. The original pictures are color images of high resolution and in JPEG format. They were turned into grayscale and reduced to the size of 256 256 pixels and were sent to the optimization model**. Figure 4** presents the raw image of the human iris, which presents the original input of the proposed image-enhancement pipeline. It represents average quality and anatomical detail that one will find in medical imaging before it undergoes any pre-processing phases. This number shows a normal distribution of texture in the iris thus making it very convenient to train and verify the effectiveness of the optimization algorithms under test. These images have been used in the whole study to design and evaluate the higher level of image-enhancement algorithms and the purpose of improving the visual appearance and clinical value of ophthalmic medical photographs.

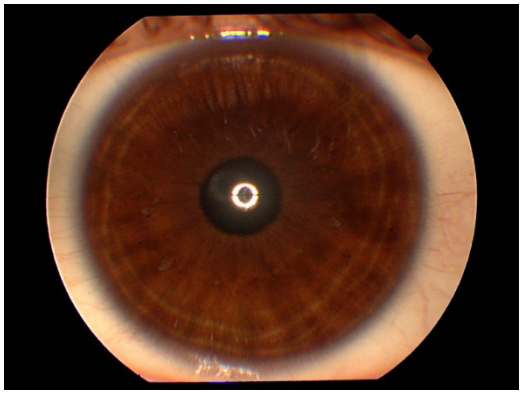

Figure 4. High-resolution image of the human iris to be used as the input in the process of preprocessing and further enhancement.

5. Result and discussion:

In this research, a series of extensive preprocessing functions were applied so as to improve the quality of the iris images before they are placed in the generative model. As shown in **Figure 2**, the process started with the configuration of the system and then the data was carefully prepared by a special pre-processing step.

5.1. Pre-processing phase: In this step, the images were to go through a carefully planned sequence of tasks that was to aim at improving their visual parameters which included contrast enhancement, attenuation of noise and enhancement of details. As demonstrated in **Figure 5**, this preprocessing pipeline where just one representative image is presented defines the manner in which each sequential operation successively enhances the image fidelity, beginning with the initial visual conditioning and ending with the crisp, artifact-free image then used in the generative model. The first was turned into grayscale in **Figure 5 (A)** thus providing consistency in processing and allowing to easily work with the features of the image in the following stages of the deep-learning process; this conversion is used to simplify the visualization and enhance the textural details of the iris (as illustrated in **Figure 5 (B)**. This was followed by the CLAHE algorithm to enhance contrast locally in order to highlight fine detail in areas where it was somewhat muted in the initial image. This effect is shown in **Figure 5 (C)**.

This was followed by applying a Bilateral filter to remove noise while preserving edge detail. This smoothed the image, as shown in **Figure 5 (D)**. In the final processing step, the Unsharp Masking technique was used to enhance sharpness in fine edges and increase the clarity of details, producing a visually more transparent image that is more ready for analysis, as shown in **Figure 5 (E)**.

It is important to note that the name "Unsharp Masking" can be misunderstood as referring to reducing sharpness. In reality, this method is used to highlight edges and clarify the image. This name comes from traditional photographic techniques, where an unsharp mask was used to enhance the localized edge contrast of the original image [45]. Therefore, despite the name, the final output is a sharpened image, which justifies its software designation in this work. The processed image is then fed into the training phase, as shown in the **Figure 2**.

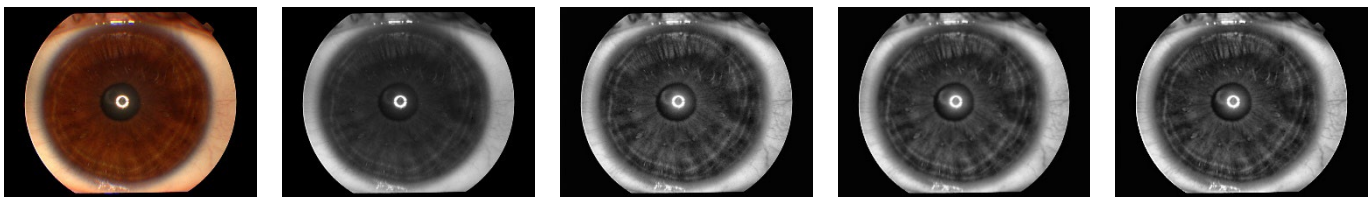

A
Original Image

B
Gray image
The original image after converting to grayscale.

C
CLHE
The result of contrast enhancement using the CLAHE algorithm.

D
Denoised (Bilateral Filter)
The result of noise removal using the Bilateral filter.

E
Sharpened (Unsharp Masking)
The result of edge sharpening using the Unsharp Masking technique.

Figure 5. Sequence of preprocessing steps for a single image from the iris database.

5.2. Model and training phase: After the preprocessing phase was over, the generative enhancement phase using a Generative Adversarial Network (GAN)-based architecture was proceeded. **Figure 3** depicts a training architecture, which combines pixel-level (L1) and perceptual (VGG) losses, which allows the generator to generate outputs that can be structurally-faithful as well as visually-coherent. The use of the Adam optimizer along with early-stopping criterion turned out to be extremely helpful in stabilizing the dynamics of the training process and avoiding overfitting. As a result, such methodological decisions produced high-quality improvement outcomes, which are supported by the visual results of the qualitative analysis and the quantitative evaluation indicators as a result.

A new generator structure was developed, with attention blocks to strengthen the medical image enhancement pipeline with an increase in fine-grained features but without affecting the natural visual structure of the input. This generator was trained with hyperparameters (lr=.0003, β_1=.7, β_2=.999). These environments were able to enhance convergence and lower the loss curve, hence train robustness. The subsequent stability had a positive effect on the quality of images, which confirms the effectiveness of the framework proposed. Compared to the standard Adam configuration (usually lr = 0.001, β_1 = 0.9, β_2 = 0.999), the chosen hyperparameter vector favors conservative updates over rapid convergence, which is fitting in the complex, non-convex optimization problems of generative models. The decreased b1 (0.7 rather than 0.9) suppresses oscillatory behavior without impairing the adaptive benefits of 0 x 2 towards its default. It has been empirically shown that this hyperparameter optimization improves training stability in GANs and with other gradient-sensitive architectures. However, the strict learning rate can increase training periods. The resultant Adam variant is therefore a trade-off between momentum-based acceleration and adaptive gradient scaling that is provide a feasible option to generative and precision discriminative tasks. Additional data augmentation methods like random rotations and horizontal flips were introduced as well to further improve generalization.

Figure 6 provides a visual comparison between original image of the grayscale iris (left) and the result obtained by the proposed framework of enhancement (right). The improved image is characterized by a better clarity of the structure and finer texture detail particularly in the central and peripheral iris. This qualitative improvement is consistent with the quantitative outcomes provided through conventional assessment parameters: the improved images reached a mean SSIM of 0.9783, LPIPS of 0.00776 and PSNR of 32.22 dB. These measurements confirm that the improvement procedure maintained perceptual and structural integrity and reduced noise and enhanced contrast, which is vital in the next diagnostic or biometric task.

5.3. Evaluation and Saving Phase: the enhanced images were evaluated quantitatively using SSIM, LPIPS, and PSNR metrics to assess both structural fidelity and perceptual quality comprehensively.

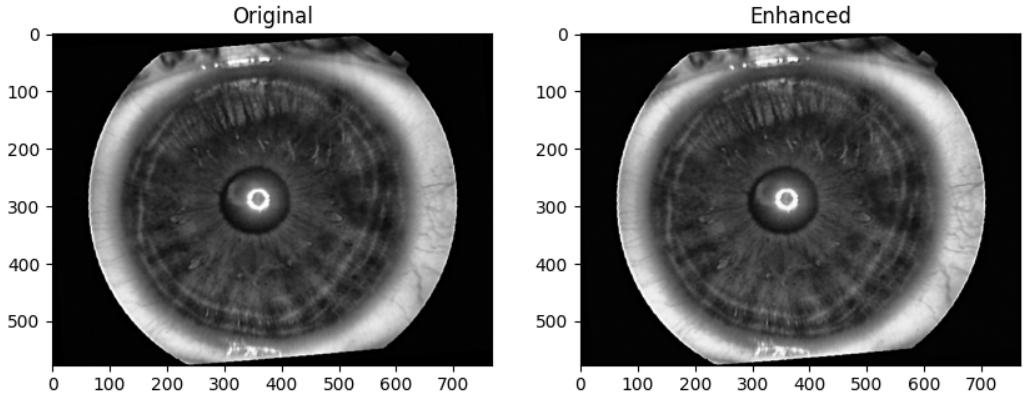

Figure 6. Comparative view of both original and improved Iris image.

As the empirical analysis of the tuned hyperparameter configuration, as reported in **Table 1**, proves, the tuned hyperparameter configuration obviously outperforms the default configuration in all three key image-quality measures: SSIM, LPIPS, and PSNR. The average SSIM has improved as 0.938347 (default) to 0.978272 (tuned). Meanwhile, LPIPS fell below 0.013732 to 0.007760, and PSNR increased to 28.6244 dB, 32.2296 dB, respectively, which correspond to improved structural fidelity, perceptual similarity and noise resilience, respectively. In addition, the decrease in standard deviation also testifies to the unchangeability of the process of improvement. SSIM STD decreased to 0.015213 and 0.044672, and this indicates that structural similarity is more stable which is essential in diagnostic reliability. Similarly, LPIPS STD decreased to 0.002139 as compared to 0.004752, which is evidence of less perceptual variation. In the case of PSNR, the standard deviation has become 2.429014 smaller than 3.587311, which supports the validity of the noise reduction and the quality of images. Taken togeth., these measures define that not only is the averaging performance increased with the tuned configuration, but also reproducible enhancement that is stable and reliable, which is a requirement of clinical imaging

applications. **Figure 7** also demonstrates the relative values of SSIM, LPIPS and PSNR over the dataset images. The figure illustrates the superiority of the model based on maximization of hyper-parameters compared to the default configuration: the value of SSIM has values approaching one, the value of LPIPS have higher magnitudes, and the value of PSNR also have higher values that are closer to zero compared to the default.

Table 1. Quantitative Evaluation Results: Standard Deviation and Average of SSIM, LPIPS, and PSNR for Enhanced Medical Images Using Tuned vs. Default Parameters.

	Hyper parameter				**Default parameter**		
	SSIM	LPIPS	PSNR		SSIM	LPIPS	PSNR
STD	0.015213	0.002139	2.429014		0.044672	0.004752	3.587311
AVERAGE	0.978272	0.00776	32.22958		0.938347	0.013732	28.6244

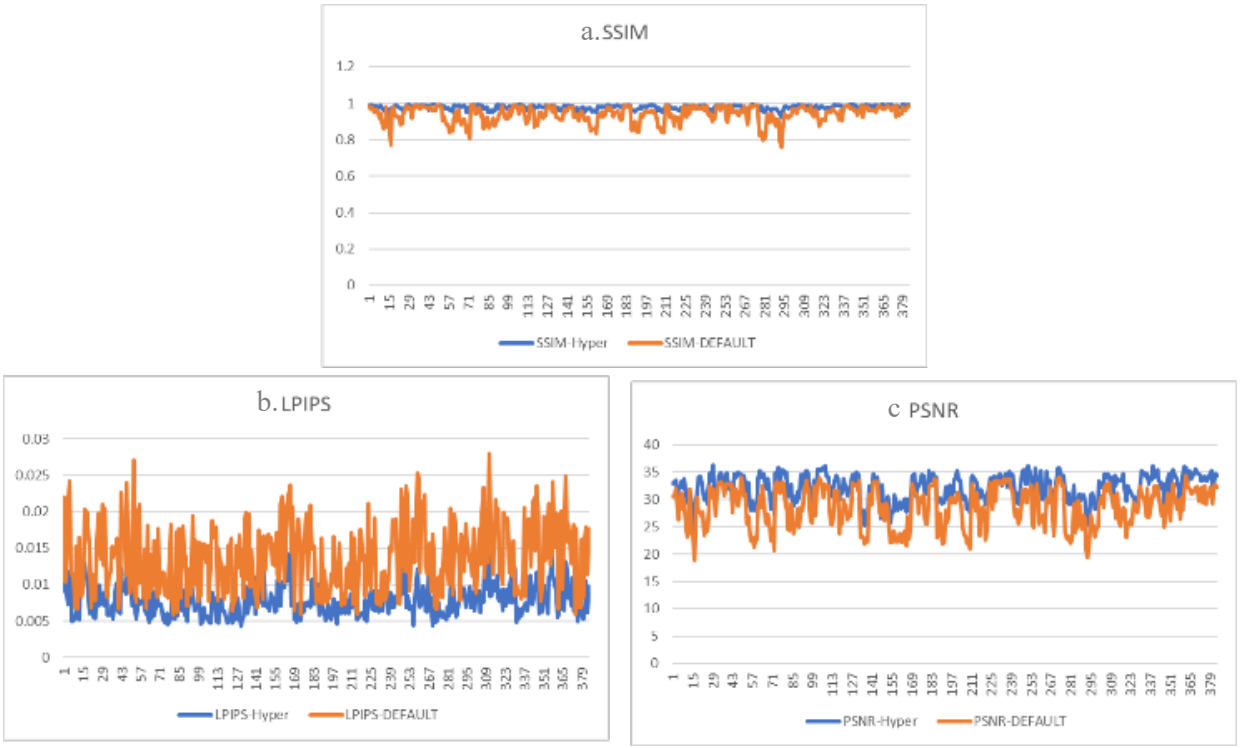

Figure 7. Quantitative comparison of three image quality metrics between default and optimized hyperparameter configurations in medical image enhancement. (a) Structural Similarity Index (SSIM): Measures how well the enhanced image accurately replicates the structural content of the original image. (b) Learned Perceptual Image Patch Similarity (LPIPS): Perceptual differences between the source image and the enhanced image; a low value means a higher quality of the image. (c) Peak Signal-to-Noise Ratio (PSNR): Is a measure of how well - clarity - the image has been enhanced; the higher the value, the lower the noise level and the higher the quality of the image on the whole.

When the findings of this study are compared to those of other studies that have been conducted before, it is clear that the proposed model has performed better. As an example, reported SSIM average the 0.978 is higher than the 0.848 reported by Mahboubisarighieh et al. 's [15] and the 0.8423 reported by Abdusalam et al.'s [16]. This enhancement highlights the increased ability of the model to achieve image texture with increased fidelity. Similarly, the PSNR has increased significantly to 32.22 dB compared to the values of 25.46 dB and 28.45 dB recorded before and hence represents

a significant decrease in the loss of information. In addition, the LPIPS value of the current model is 0.00776 which is much lower than the value 0.152 measured in the work by Mahboubisarighieh et al.'s which proves the large improvement in the quality of visual perception. All these comparisons illustrate that the proposed model is excellent in terms of optical and structural efficiency, thus increasing its possibilities of application in precision medicine.

Conclusion

The given research has offered a novel GAN-based system to improve medical images, specifically, to enhance the quality of diagnostic images by introducing a carefully designed preprocessing pipeline and a tailored training process. The sequential processing system has helped in the improvement of the quality of images, thus increasing the quality of disease diagnosis based on image analysis. The findings suggest that hyperparameter optimization has led to notable improvements in the performance in terms of key assessment metrics, with an average SSIM of 0.9783, an LPIPS of 0.00776, and a PSNR of 32.22dB being superior to default settings and other state-of-the-art results. In addition, the lower standard deviations (SSIM STD = 0.0152, LPIPS STD = 0.0021, PSNR STD = 2.4290) indicate the increased stability and accuracy of the quality of the output. The results emphasize the need to be careful about hyperparameter optimization and employ loss functions that are targeted in achieving reliable, high-fidelity medical image enhancement that would be applicable in clinical practice. Future studies can also be aimed at enhancing the functionality of deep learning methodologies to attain a complete coverage that can be extrapolated to all medical imaging modalities and incorporate the artificial intelligence networks into the preprocessing phase.

Acknowledgement

The author would like to express they're thanks to the College of Computer Sciences and Mathematics, University of Mosul, for their support of this paper.

Conflict of interest

None.

References

[1] A. Suman, P. Suman, S. Padhy, N. Kumar and A. Sing, "Healthcare revolution: Advances in AI-driven medical imaging and diagnosis," Responsible and Explainable Artificial Intelligence in Healthcare, pp. 155-182, 2025. https://doi.org/10.1016/B978-0-443-24788-0.00007-8

[2] A. Haleem, M. Javaid, R. P. Singh and R. Suman, "Medical 4.0 technologies for healthcare: Features, capabilities, and applications," Internet of Things and Cyber-Physical Systems, vol. 2, pp. 12-30, 2022. https://doi.org/10.1016/j.iotcps.2022.04.001 .

[3] K. J. Zuiderveld, "Contrast limited adaptive histogram equalization," Graphics gems, vol. 4, no. 1, pp. 474-485, 1994. https://doi.org/10.1016/b978-0-12-336156-1.50061-6 .

[4] A. N. Younis and F. M. Ramo, "Detecting Skin Cancer Disease Using Multi Intelligent Techniques," International Journal of Mathematics and Computer Science, vol. 16, no. 4, pp. 1783-1789, 2021.

[5] Y. Ma, J. Liu, Y. Liu, H. Fu, Y. Hu, J. Cheng and Y. Zhao, "Structure and illumination constrained GAN for medical image enhancement," IEEE Transactions on Medical Imaging, vol. 40, no. 12, pp. 3955-3967, 2021. https://doi.org/10.1109/tmi.2021.3101937

[6] F. Spagnolo, P. Corsonello, F. Frustaci and S. Perri, "Design of approximate bilateral filters for image denoising on FPGAs," IEEE Access, 2023. https://doi.org/10.1109/access.2022.3233921

[7] M. K. K. Masood, E. N. Baro and P. O. Roth, " A Novel Intensity-Corrected Blue Channel Compensation and Edge-Preserving Contrast Enhancement Using Laplace Filter and Sigmoid Function for Sand-Dust Image Enhancement," IEEE Access, 2025. https://doi.org/10.1109/access.2025.3548972

[8] Z. Zhang, A. J. Yezzi and G. Gallego, "Formulating event-based image reconstruction as a linear inverse problem with deep regularization using optical flow," IEEE Transactions on Pattern Analysis and Machine Intelligence, vol. 45, no. 7, pp. 8372-8389, 2022. https://doi.org/10.1109/tpami.2022.3230727

[9] N. Seliya, A. A. Zadeh and T. M. Khoshgoftaar, "A literature review on one-class classification and its potential applications in big data," Journal of Big Data,2021. https://doi.org/10.1186/s40537-021-00514-x

[10] A. N. Bishop and P. Del Moral, "On the mathematical theory of ensemble (linear-Gaussian) Kalman–Bucy filtering," Mathematics of Control, vol. 35, no. 4, pp. 835-903, 2023. https://doi.org/10.1007/s00498-023-00357-2

[11] S. Sharif, R. A. Naqv, M. Biswa and W.-K. Loh, "Deep Perceptual Enhancement for Medical Image Analysis," IEEE Journal of Biomedical and Health Informatics, vol. 26, no. 10, pp. 4826-4836, 2022. https://doi.org/10.1109/jbhi.2022.3168604

[12] K. G. Dhal, A. Das, S. Ray, J. Gálvez and S. Das, "Histogram equalization variants as optimization problems: a review," Archives of Computational Methods in Engineering, vol. 28, pp. 1471-1496, 2021. https://doi.org/10.1007/s11831-020-09425-1

[13] I. S. Mohammed and M. K. Hussien, "Off-line handwritten signature recognition based on genetic algorithm and Euclidean distance," IAES International Journal of Artificial Intelligence, vol. 12, no. 3, p. 1238~1249, 2023. https://doi.org/10.11591/ijai.v12.i3.pp1238-1249

[14] V. Sampath, I. Maurtua, J. J. A. Martin and A. Gutierrez, "A survey on generative adversarial networks for imbalance problems in computer vision tasks," Journal of Big Data vol. 8, no. 27, 2021. https://doi.org/10.1186/s40537-021-00414-0

[15] A. Mahboubisarighieh, H. Shahverdi, S. J. Nesheli, M. A. Kermani, M. Niknam, M. Torkashvand and S. M. Rezaeijo, "Assessing the efficacy of 3D Dual-CycleGAN model for

multi-contrast MRI synthesis," Egyptian Journal of Radiology, vol. 55, no 118, 2024. https://doi.org/10.1186/s43055-024-01287-y

[16] A. Abdusalomov, S. Mirzakhalilov, Z. Dilnoza, K. Zohirov, R. Nasimov, S. Umirzakova and Y. Cho, "Lightweight Super-Resolution Techniques in Medical Imaging: Bridging Quality and Computational Efficiency," Bioengineering (Basel), vol. 11, no. 12, 2024. https://doi.org/10.3390/bioengineering11121179

[17] P. Pawar, B. Ainapure, M. Rashid, N. Ahmad, A. Alotaibi and S. S. Alshamrani, "Deep learning approach for the detection of noise type in ancient images," Sustainability, vol. 14, no. 18, p. 11786, 2022. https://doi.org/10.3390/su141811786

[18] M. Momeny, A. M. Latif, M. A. Sarram, R. Sheikhpour and Y. D. Zhang, "A noise robust convolutional neural network for image classification," Results in Engineering, vol. 10, p. 100225, 2021. https://doi.org/10.1016/j.rineng.2021.100225

[19] V. D. P. Jasti, A. S. Zamani, K. Arumugam, M. Naved, H. Pallathadka and F. Sammy, "Computational technique based on machine learning and image processing for medical image analysis of breast cancer diagnosis," Security and communication networks, vol. 2022, no. 1, p. 1918379, 2022. https://doi.org/10.1155/2022/1918379

[20] S. Guo, M. Li, Y. Li, J. Chen, H. K. Zhang, L. Sun, Wang J., Wang R. and Y. Yang, "The improved U-STFM: a deep learning-based nonlinear spatial-temporal fusion model for land surface temperature downscaling," Remote Sensing, vol. 16, no. 2, p. 322, 2024. https://doi.org/10.3390/rs16020322

[21] R. Sepasdar, A. Karpatne and M. Shakiba, "A data-driven approach to full-field nonlinear stress distribution and failure pattern prediction in composites using deep learning," Computer Methods in Applied Mechanics and Engineering, vol. 397, p. 115126, 2022. https://doi.org/10.1016/j.cma.2022.115126

[22] Z. Chen, K. Pawar, M. Ekanayake, C. Pain, S. Zhong and G. F. Egan, "Deep learning for image enhancement and correction in magnetic resonance imaging—state-of-the-art and challenges," Journal of Digital Imaging, vol. 36, pp. 204-230, 2 2023. https://doi.org/10.1007/s10278-022-00721-9

[23] I. M. Mohammed and N. A. M. Isa, "Contrast Limited Adaptive Local Histogram Equalization Method for Poor Contrast Image Enhancement," IEEE Access, vol. 13, pp. 62600 - 62632, 2025. https://doi.org/10.1109/access.2025.3558506

[24] A. Fawzi, A. Achuthan and B. Belaton, "Adaptive clip limit tile size histogram equalization for non-homogenized intensity images," IEEE Access vol. 9, pp. 164466 - 164492, 2021. https://doi.org/10.1109/access.2021.3134170

[25] J. Liu, X. Zhou, Z. Wan, X. Yang, W. He, R. He and Y. Lin, "Multi-scale FPGA-based infrared image enhancement by using RGF and CLAHE," Sensors, vol. 23, no. 19, 2023. https://doi.org/10.3390/s23198101

[26] M. M. Khattab, A. M. Zeki, A. A. Alwan, B. Bouallegue, S. S. Matter and A. M. Ahmed, "Regularized Multiframe Super-Resolution Image Reconstruction using Linear and Nonlinear Filters," Journal of Electrical and Computer Engineering, vol. 2021, no. 1, p. 8309910, 2021. https://doi.org/10.1155/2021/8309910

[27] P. Lu and Q. Huang, "Robotic weld image enhancement based on improved bilateral filtering and clahe algorithm," Electronics, vol. 11, no. 21, 2022. https://doi.org/10.3390/electronics11213629

[28] H. Li and X. L. Duan, "SAR ship image speckle noise suppression algorithm based on adaptive bilateral filter," Wireless Communications and Mobile Computing, vol. 2022, no. 1, p. 9392648, 2022. https://doi.org/10.1155/2022/9392648

[29] J. Mao, Z. Wu and X. Feng, "Image definition evaluations on denoised and sharpened wood grain images," Coatings, vol. 11, no. 8, 2021. https://doi.org/10.3390/coatings11080976

[30] H. A. Jalab, M. A. Alqarni, R. W. Ibrahim and A. A. Almazroi, "A novel pixel's fractional mean-based image enhancement algorithm for better image splicing detection," Journal of King Saud University-Science, vol. 34, no. 2, p. 101805, 2021. https://doi.org/10.1016/j.jksus.2021.101805

[31] Y. Wang and J.J. Healy, " Image Quality Assessment for Gibbs Ringing Reduction," Algorithms, vol. 16, no. 2, 2023. **https://doi.org/10.3390/a16020096**

[32] X. Yi, E. Walia and P. Babyn, "Generative Adversarial Network in Medical Imaging: A Review," Medical Image Analysis, vol. 58, 2019. https://doi.org/10.1016/j.media.2019.101552

[33] R. K. Remya, K. R. Vidya and M. Wilscy, "Detection of deepfake images created using generative adversarial networks: A review." Second International Conference on Networks and Advances in Computational Technologies: NetACT 19. Cham: Springer International Publishing, pp. 25-35, 2021.

[34] E. Strelcenia and S. Prakoonwit, "A survey on GAN techniques for data augmentation to address the imbalanced data issues in credit card fraud detection," Machine Learning and Knowledge Extraction, vol. 5, no. 1, 2023. https://doi.org/10.3390/make5010019

[35] A. Figueira and B. Vaz, "Survey on synthetic data generation, evaluation methods and GANs," Mathematics, vol. 10, no. 15, 2022. https://doi.org/10.3390/math10152733

[36] M. M. Sanja, Z. Lukac and M. Temerinac. "Objective estimation of subjective image quality assessment using multiparameter prediction," IET Image Processing, vol. 13, no. 13, 2019. **https://doi.org/10.1049/iet-ipr.2018.6143**

[37] A.M. Adeshina, S. Abdul Razak, S. Yogarayan and M. S. Sayeed "Measuring Fidelity of Steganography Approach in Securing Clinical Data Sharing Platform using Peak Signal to Noise Ratio (PSNR) and Structural Similarity Index Measure (SSIM)," *Informatica, vol.* 49, no. 11, 2025. https://doi.org/10.31449/inf.v49i11.5661

[38] V. Mudeng, M. Kim and S. Choe, "Prospects of structural similarity index for medical image analysis," Applied Sciences, 2022.

https://doi.org/10.3390/app12083754

[39] O. Sjögren, G. G. Pihlgren, F. Sandin and M. Liwicki, "Identifying and Mitigating Flaws of Deep Perceptual Similarity Metrics, Proceedings of the Northern Lights Deep Learning Workshop 2023", vol. 4, 2023. https://doi.org/10.7557/18.6795

[40] S. Czolbe, P. Pegios, O. Krause and A. Feragen, " Semantic similarity metrics for image registration ," Medical Image Analysis, vol.. 87, no. 102830, 2023, https://doi.org/10.1016/j.media.2023.102830

[41] X. Sun, N. Gazagnadou, V. Sharma, L. Lyu, H. Li and L. Zheng " Privacy Assessment on Reconstructed Images: Are Existing Evaluation Metrics Faithful to Human Perception?," 37th Conference on Neural Information Processing Systems (NeurIPS 2023), vol. 36, pp. 10223--10237, 2023.

[42] M. Arabboev, S. Begmatov, M. Rikhsivoev, K. Nosirov and S. Saydiakbarov, "A comprehensive review of image super-resolution metrics: classical and AI-based approaches," *Acta IMEKO*, vol. *13, no. 1, pp.* 1-8, 2024. https://doi.org/10.21014/actaimeko.v13i1.1679

[43] Z. Shu and K. Zhang, "Spectral Normalization for Generative Adversarial Networks for Artistic Image Transformation", International Journal of Digital Multimedia Broadcasting, vol. 1, 2024. https://doi.org/10.1155/2024/6644706

[44] M. Dobeš and L. Machala, "Iris Database," 2002. [Online]. Available: http://phoenix.inf.upol.cz/iris/.

[45] R. C. Gonzalez and R. E. Woods, Digital Image Processing (4th ed.), Pearson, 2018.